


ORIGINAL
ARTICLENeuronal *KIF5b* deletion induces *striatum*-dependent locomotor impairments and defects in membrane presentation of dopamine D2 receptors

Lucas E. Cromberg*, Trinidad M. M. Saez*†, María G. Otero*, Eugenia Tomasella†, Matías Alloatti*, Ana Damianich‡§, Victorio Pozo Devoto¶, Juan Ferrario‡, Diego Gelman†, Marcelo Rubinstein§** and Tomás L. Falzone*† 

**Instituto de Biología Celular y Neurociencias IBCN (CONICET-UBA), Facultad de Medicina, Universidad de Buenos Aires, Buenos Aires, Argentina*

†*Instituto de Biología y Medicina Experimental IBYME (CONICET), Buenos Aires, Argentina*

‡*Instituto de Investigaciones Farmacológicas ININFA, (CONICET-UBA), Buenos Aires, Argentina*

§*Instituto de Investigaciones en Ingeniería Genética y Biología Molecular INGEBI (CONICET), Buenos Aires, Argentina*

¶*Center for Translational Medicine (CTM), International Clinical Research Center, St. Anne's University Hospital (ICRC-FNUSA), Brno, Czech Republic*

***Facultad de Ciencias Exactas y Naturales, Universidad de Buenos Aires, Buenos Aires, Argentina*

Abstract

The process of locomotion is controlled by fine-tuned dopaminergic neurons in the *Substantia Nigra pars-compacta* (*SNpc*) that projects their axons to the dorsal *striatum* regulating cortical innervations of medium spiny neurons. Dysfunction in dopaminergic neurotransmission within the *striatum* leads to movement impairments, gaiting defects, and hypo-locomotion. Due to their high polarity and extreme axonal arborization, neurons depend on molecular motor proteins and microtubule-based transport for their normal function. Transport defects have been associated with neurodegeneration since axonopathies, axonal clogging, microtubule destabilization, and lower motor proteins levels were described in the brain of patients with Parkinson's Disease and other neurodegenerative disorders. However, the contribution of specific motor proteins to the regulation of the nigrostriatal network remains unclear. Here, we generated different conditional knockout mice for the kinesin heavy chain 5B subunit (*Kif5b*) of Kinesin-1 to unravel its contribution to locomotion. Interestingly, mice with

neuronal *Kif5b* deletion showed hypo-locomotion, movement initiation deficits, and coordination impairments. High pressure liquid chromatography determined that dopamine (DA) metabolism is impaired in neuronal *Kif5b*-KO, while no dopaminergic cell loss was observed. However, the deletion of *Kif5b* only in dopaminergic neurons is not sufficient to induce locomotor defects. Noteworthy, pharmacological stimulation of DA release together with agonist or antagonist of DA receptors revealed selective D2-dependent movement initiation defects in neuronal *Kif5b*-KO. Finally, sub-cellular fractionation from *striatum* showed that *Kif5b* deletion reduced the amount of dopamine D2 receptor in synaptic plasma membranes. Together, these results revealed an important role for *Kif5b* in the modulation of the striatal network that is relevant to the overall locomotor response.

Keywords: axonal transport, dopamine, dopamine receptors, *Kif5b*, locomotor response, nigrostriatal pathway.

J. Neurochem. (2019) **149**, 362–380.

Received May 17, 2018; revised manuscript received August 27, 2018; accepted January 11, 2019.

Address correspondence and reprint requests to Tomás L. Falzone, IBCN (CONICET-UBA), Paraguay 2155, Buenos Aires C1121ABG, Argentina. E-mail: tfalzone@fmed.uba.ar

Abbreviations used: APP, amyloid precursor protein; DIR, dopamine receptor D1; D2R, dopamine receptor D2; DA, dopamine; DAK5b-KO,

Kif5b^{loxP/loxP}; *Dat*^{+/-ires-cre} mice; DArgic, dopaminergic; HPLC, high pressure liquid chromatography; KHC, kinesin heavy chain; *Kif5b*, kinesin heavy chain 5B subunit; MAO, monoamine oxidase; MSN, medium spiny neurons; NeuK5b-KO, *Kif5b*^{loxP/loxP}; Tg.(Nes-cre) mice; PD, Parkinson disease; RRID, research resource identifier (see sci-crunch.org); *SNpc*, *substantia nigra pars compacta*.

A variety of neurological disorders associated with defects in the stimulation of *striatal* medium spiny neurons convey in the clinical manifestation of motor symptoms, such as bradykinesia and locomotor impairments (Spillantini *et al.* 1997; Fahn 2003). The function of *substantia nigra pars compacta* dopaminergic (DAergic) neurons, with ramified axons covering 6% of the neostriatum, depend on a regulated axonal transport system (Matsuda *et al.* 2009). Defects in vesicle and organelle distribution found in dystrophic neurites have been proposed to occur in Parkinson disease (PD) due to cytoskeletal disruptions induced by α -synuclein and tau protein accumulation in Lewy deposits and neurofibrillary tangles, respectively (Braak and Braak 1990; Abeliovich and Gitler 2016; Volpicelli-Daley 2017). In addition, different PD models developed early axonal transport impairments prior to the neurodegenerative process (Chu *et al.* 2012; Lu *et al.* 2014; Pozo Devoto *et al.* 2017).

Molecular motors transport cargos along polarized microtubules in an anterograde and retrograde manner (De Vos *et al.* 2008). Kinesin-1 is a plus-end microtubule motor composed of two kinesin heavy chains (KHC), which interact with microtubules, and two light chains that associate with cargo (Vale *et al.* 1985). Three genes coding for KHC are expressed in mammals (*Kif5a*, *Kif5b*, and *Kif5c*) (Miki *et al.* 2001). *Kif5b* is ubiquitously expressed, whereas *Kif5a* and *Kif5c* are enriched in neurons (Kanai *et al.* 2000). Kif5 subunits have been initially considered redundant and responsible for the transport of mitochondria (Tanaka *et al.* 1998; Kanai *et al.* 2000), amyloid precursor protein (APP) vesicles (Kamal *et al.* 2000), GABA receptors (Twelvetrees *et al.* 2011; Nakajima *et al.* 2012), and lysosomes (Tanaka *et al.* 1998). However, different studies have suggested functional differences between Kif5 subunits (Deboer *et al.* 2009). Mutant mice with constitutive *Kif5a* deletion die at birth (Xia *et al.* 2003), whereas its conditional removal from neurons impairs GABA receptor and neurofilament transport generating severe epilepsy, and postnatal death (Twelvetrees *et al.* 2011). Mice lacking *Kif5c* develop a smaller brain, but no other differential phenotype has been described (Kanai *et al.* 2000). Mice without *Kif5b* expression are embryonic lethal due to defects in mitochondria and lysosome dispersion in non-neuronal cells (Tanaka *et al.* 1998). Therefore, the contribution of different motors to the function of specific neuronal pathways, and their role in locomotion remains elusive.

The central neuronal loop that controls locomotion and coordination in mammals involves cortical neurons projecting to the *striatum* which is regulated by nigral DAergic innervations (Bolam, 2000). GABAergic medium spiny neurons (MSN) in the *striatum* are divided in direct and indirect pathways (Mink 2003). Direct pathway neurons express dopamine D1 receptors (DIR) and promote

movement (Gerfen *et al.* 1990; Mink 2003). Oppositely, indirect pathway neurons express dopamine D2 receptors (D2R) and inhibit movement (Gerfen *et al.* 1990; Mink 2003). Their coordinated activity is required for movement generation and fine tune locomotion processes (Cui *et al.* 2014). Consequently, pharmacological blockade of D1R by antagonist SCH 23390 has been described to inhibit movement; similar to the effect of D2R agonist quinpirole (Starr and Starr 1986; Usiello *et al.* 2000). D2R deletion in mice leads to hypo-locomotion, indicating that activation of this neurons is essential for movement (Baik *et al.* 1995; Kelly *et al.* 1998). Although D1R and D2R are actively transported within neurons (van Der Kooy *et al.* 1986; Aiso *et al.* 1987) the contribution of specific motor protein to their transport have been unexplored. Moreover, the motor protein responsible for the intracellular distribution of dopamine (DA)-related cargos, and their role in locomotion remain elusive.

Here we aim to elucidate the role of Kif5b in the nigrostriatal pathway. Our data reveal that Kif5b plays essential roles in regulating *striatum*-dependent locomotion by modulating DA metabolism and D2R presentation at the plasma membrane.

Materials and methods

Animals

Mice were housed in 24°C temperature- and 12 h light/dark-controlled rooms with *ad libitum* food and water access. Experiments with animals were performed following approved university protocols (UBA-456/2010). *Kif5b^{loxP/loxP}* mice were obtained from NIH-NCI (MTA:33287-11) (Cui *et al.* 2011) and crossed with Tg.(Nes-cre) mice (IMSR Cat# JAX:003771, research resource identifier, RRID:IMSR_JAX:003771) (Tronche *et al.* 1999) or *Dat^{+/-ires-cre}* mice (IMSR Cat# JAX:006660, RRID:IMSR_JAX:006660) (Bäckman *et al.* 2006) in C57BL/6J background. *Kif5b^{+/-loxP}*;Tg.(Nes-cre) crossed with *Kif5b^{loxP/loxP}* bred to produced offspring with *Kif5b^{loxP/loxP}*, *Kif5b^{+/-loxP}*;Tg.(Nes-cre), and *Kif5b^{loxP/loxP}*;Tg.(Nes-cre) genotypes. *Kif5b^{+/-loxP}*; *Dat^{+/-ires-cre}* crossed with *Kif5b^{loxP/loxP}* bred to produced offspring with *Kif5b^{loxP/loxP}*, *Kif5b^{+/-loxP}*; *Dat^{+/-ires-cre}*, and *Kif5b^{loxP/loxP}*; *Dat^{+/-ires-cre}* genotypes. Genotypification was performed from DNA extracted from ear punches using primers *loxP*: forward: 5'TGAAGGCTAAGTCAGATATGGATGC3', reverse 1: 5'GGATTGGCACCTTTACCTAGAAGG3' and reverse 2: 5'TTA CTAACCTGAACCTGGCTTCCTAG3'; for detecting *Cre* in Tg.(Nes-cre) forward: 5'GCATAACCAGTGAAACAGCATG CTG3', reverse: 5'AAAATTTGCCTGCATTACCG3'; for *Cre* in *Dat^{+/-ires-cre}* forward: 5'TGGCTGTTGGTGTAAAGTGG3', IRES: 5'CCAAAAGACGGCAATATGGT3' and reverse: 5'GGACA GGGACATGGTTGACT3'. PCR parameters were: 95°C-5 min, followed by 35 cycles of 95°C-30 s, 55°C-30 s, and 72°C-1 min and last round at 72°C-5 min. Behavioral tests were performed during light period in a dimmed illuminated room at 24°C after habituating mice for 1 h. Timeline used for animal testing and number of mice on each experiment is described in figures. Mice

were killed by CO₂ inhalation in a chamber following approved protocols. Total number of mice used per genotypes is: *Kif5b^{loxP/loxP}* 104, *NeurK5b-KO* 88, *Kif5b^{loxP/loxP};Dat^{+/-ires-cre}* mice (DAK5b-KO): 18. Arbitrary selection was performed to allocate drug or saline treatment. No animal tested was excluded from analysis.

Open field

Mice were allowed to freely explore a chamber (50 × 50 cm) for 30 min while being recorded and videos analyzed using ANY-maze software (Version 4.3; Stoelting Co., Wood Dale, IL, USA). The total distance travelled, the number of initiation episodes and the time taken for moving in the center (16.5 × 16.5 cm centered square) were noted down. Movement initiation was quantified when a still mouse (immobile for more than 2 s) made a change in position of more than 20% of the pixels representing its body. Mouse behavior represented by grooming and rearing were quantified from movies.

Gaiting analysis

To perform the step analysis mice were allowed to freely walk over a blotting paper in a straight narrow half-tube (30 cm) after their paws were stained with black ink to generate footprints. Distances between left and right footprints and inter-limb distances were analyzed.

Rotarod

Rotarod assay was performed in two consecutive days in which mice were trained and tested in two trials of 10 min spaced 2 h in between. Rod speed was constant at 14 rpm. Number of falls and maximum time over the rod were registered.

Plus maze

Mice were placed in the center of an elevated plus maze (50 cm in height) composed of two open and two closed arms (5 × 30 cm). Mice were allowed to freely walk for 5 min and tracked using ANY-maze software. Proportion of time spent in arms and number of entries to arms was measured.

Drugs

D-amphetamine (Sigma, St Louis, MO, USA, A3278; 7.5 mg/kg) dissolved in phosphate-buffered saline (PBS) was administered intraperitoneally 15 min before testing. SCH 23390 (0.25 mg/kg; Santa Cruz Biotechnology, Santa Cruz, CA, USA, 125941-87-9) or Quinpirole hydrochloride (0.05 mg/kg; Santa Cruz Biotechnology, 85798-08-9) were administered 15 min prior D-amphetamine administration (30 min before Open Field test).

High-performance liquid chromatography

Striatum was dissected and frozen at -80°C. Dissected *striatum* was weighed, homogenized, and deproteinized in perchloric acid (HClO₄ 0.2N, 1/40 w/vol). Homogenates were centrifuged (13000 g, 7 min) and supernatants injected in a NOVA-PAK C18 3.9 × 150 mm column, with PicB8 4.8 mL, NaH₂PO₄H₂O 10.8 g, EDTA (0.99 mM) and 72 mL methanol as mobile phase. Chromatography was done with the Peak Simple Chromatography data system equipment, voltage measured with Amperometric Detector LC 48

(BASi, West Lafayette, IN, USA). Pick Easy software (SRI instruments, Bad Honnef, Germany) was used to analyze intensity voltage peaks and concentrations.

Histology

Killed mice were rapidly subjected to a transcardial perfusion by injecting a butterfly needle in the left ventricle coupled to a peristaltic pump. 20 mL of PBS pH: 7.4 was perfused at a pace of 1.5 mL/min following with 20 mL of 4% paraformaldehyde in PBS. After fixation, mice were decapitated with scissors, the skin removed from the head, the skull cut laterally and at the middle from posterior to anterior using fine scissors. Both parietal bones were broken off to release the brain, which was carefully removed and placed overnight in 4% paraformaldehyde in PBS solution at 4°C. Next day brains were changed to 20% sucrose solution (O/N). Brains mounted in freezing media (OCT) were coronally sectioned (50 μm) using a cryostat (Leica CM1850). Brain slices were put sequentially in 6 wells to obtain the brain representation in each well containing 10 sections spaced apart by 300 μm. For immunohistochemistry brain slices were blocked (1 h in 10% goat serum in phosphate saline buffer, 0.5% triton, at 24°C) and incubated with primary antibodies O/N (16 h, 10% goat serum in PBS, 0.5% triton, at 4°C). Secondary biotinylated antibody (1 : 300; Jackson Immuno-Research, West Grove, PA, USA, Goat anti-rabbit IgG 111-065-003, Goat anti-mouse IgG 115-065-003) and streptavidine-peroxidase amplification was performed, followed by diaminobenzidine development kit (Vector Laboratories, Burlingame, CA, USA). Images were acquired using a 40× lens on an Olympus IX81 microscope (Olympus, Tokio, Japan). Volume analysis were estimated from brain, ventricles, and cortex using seven arbitrary selected systematic serial sections of 50 μm slices spaced apart by 300 μm. Cavalieri's principle was used for unbiased estimation of an arbitrary shape volume. $V_{\text{Cavalieri}} = t (A_1 + A_2 + \dots + A_p)$. Volumes were obtained from the product of the distance between analyzed planes (*t*) and the sum of registered areas on systematic-arbitrary sections (Falzone *et al.* 2009).

Reverse transcription PCR (RT-PCR)

Dissected *striatum* from mice was lysed in trizol and mRNA extracted for cDNA transcription with Transcriptor First Strand cDNA Synthesis Kit (Roche Molecular Biochemicals, Indianapolis, IN, USA). RT-PCR was performed for DRD2 using primer forward: 5'CCACACTGGTTATGCCCTGG3'; reverse: 5'GGTTCAAGATGCTTGCTGTGC3'; DRD1, forward: 5'GATGGCTCCTAACACTTCTACC3'; reverse: 5'GGCTGTGAGGATGCGAAAAG3' Cyclofilin, forward: 5'TGGAGATGAATCTGTAGGACGA3'; reverse: 5'GAA GTCTCCACCCTGGATCA3'. PCR parameters were: 95°C-10 min, followed by 40 cycles of 95°C-15 s, 60°C-1 min, and 72°C-1 min and last round at 72°C-5 min.

Synaptic membrane purification

Homogenized *striatum* from three mice per genotype were maintained at 4°C (0.3 M sucrose, 4 mM HEPES pH 7.5, protease inhibitors) and centrifuged (1000 g, 10 min) to obtain P1 pellet and S1 supernatant (cytosolic fraction). P2 and S2 were obtained by further centrifugation of S1 (9200 g, 15 min). A similar procedure was repeated to obtain P2' (crude synaptosomes) which was resuspended in similar initial volume of HEPES buffer and subjected to hypotonic shock with nine additional volumes of cold water. After 10 min, buffer and pH was recovered

using 1 M HEPES pH 7.5. Synaptic vesicles (LS1) and synaptic plasma membrane (LP1) fractions were obtained by centrifugation (25 000 g, 20 min). 30 µg of protein were loaded in each fraction for western blots that were developed using standard enhanced chemiluminescence (Thermo) procedures.

Antibodies

Tyrosine hydroxylase (TH) rabbit (Millipore Corporation, Bedford, MA, USA, AB152, RRID:AB_390204; IF1/600), Kif5b rabbit (Purified serum; IF 1/200, WB 1/500), KHC mouse (Millipore Corporation, MAB1614, RRID:AB_94284; WB 1/500), tubulin mouse (Millipore Corporation, DM1α 05-829; 1/10000), NMDAR rabbit (Sigma-Aldrich, St. Louis, MO, USA, G8913, RRID:AB_259978, WB 1/1000), D2R rabbit (WB 1/200). HOMER rabbit (Synaptic Systems, Göttingen, Germany, 160003, RRID:AB_887730, WB 1/1000). Secondary fluorescent antibodies from molecular probes alexa conjugated to 488 (Thermo-Fisher, Goat anti-rabbit IgG A11034, Goat anti-mouse IgG A28175) and 565 (Thermo Fisher, Waltham, MA, USA, Goat anti-rabbit IgG A11011, Goat anti-mouse IgG A11004) were used 1/500. Alkaline phosphatase conjugated secondary antibodies were used in WB 1 : 10 000 (Jackson Immuno-Research, Goat anti-rabbit IgG 111-035-144, Goat anti-mouse IgG 115-035-146).

Primary hippocampal cell culture

Hippocampi from newborn mice were dissected and incubated in a 0.22-mm-filtered mixture A solution (45 U papain, 0.05% DNase in PBS) for 20 min at 37°C and then triturated by pipetting. Cells were grown (500 mM L-glutamine, Neurobasal + B27) over poly-D-lysine-coated coverslips (37°C, 5% CO₂) (Falzone and Stokin 2012). Plasmid pcdna3 CMV-APP-yellow fluorescent protein (YFP) containing a protein fusion between APP695 and YFP, and plasmid pcdna3 CMV-MITO-EGFP containing the enhanced green fluorescent protein (EGFP) fused to a mitochondrial signal peptide from the human cytochrome C were transfected in neurons at a low transfection efficiency (5–10%) using Lipofectamine 2000 (Invitrogen) (Falzone *et al.* 2009).

Movie acquisition and kymograph analysis

APP-YFP and MITO-EGFP were recorded using an inverted epifluorescent microscope connected to a CCD camera (Olympus IX81-DP71/12.5) and a 60× lens (NA: 1.40) with a heating chamber (5% CO₂, 37°C) (Tokai). Directionality was determined by tracking axons 2 fields away from cell bodies or projection tips. Continuous 30-s stacks (224 frames) at 125 msec/frame (8 Hz) were collected for APP-YFP or time lapse (1 frame/2 s) for MITO-EGFP. Kymographs were plotted with Image J (NIH, Bethesda, MD, USA) using multiple-kymograph plug-in, and particle proportion, average velocities and density extracted (Falzone and Stokin 2012).

Experimental design and statistical analysis

Sample size in behavioral experiments was calculated using the mean difference between two groups following protocols performed previously (Rubinstein *et al.* 1997; Falzone *et al.* 2002). Averages were plotted in graphs and bars represented standard error of the mean (SEM). Data were assessed for normal distribution prior analysis using Shapiro–Wilk normality test. Statistical analysis was performed using Student's *t*-test with

independent two tails when comparing two groups, or two-way ANOVA followed by Bonferroni post hoc test when variables (genotype and treatment) were analyzed simultaneously. No test to identify outliers was performed. GraphPad Prism Software was used for analysis (Windows 7.00; La Jolla, CA, USA). Asterisks indicate significance.

Results

Mice lacking neuronal *Kif5b* motor protein survive and develop a normal brain

Since constitutive deletion of *Kif5b* in mice resulted in embryonic lethality (Tanaka *et al.* 1998), its contribution to neuronal function remains elusive. To dissect the neuronal role of Kif5b in locomotion we selectively deleted its expression from neurons by the Cre-*loxP* system. Mice with *Kif5b* exon 2 flanked by *loxP* sites (*Kif5b^{loxP/loxP}*) were crossed with transgenic mice expressing Cre recombinase under the nestin promoter, Tg(Nes-cre) (Tronche *et al.* 1999; Cui *et al.* 2011) (Fig. 1a). From our breeding strategy we obtained mice with the conditional genomic deletion of *Kif5b* in neurons (*Kif5b^{loxP/loxP}*;Tg.Nes-cre, from now on: NeurK5b-KO), mice with one deleted *Kif5b* allele in neurons (*Kif5b^{+loxP}*;Tg.Nes-cre) and control mice (*Kif5b^{loxP/loxP}*) (Fig. 1b). Cre-mediated recombination in neurons was tested by crossing Tg(Nes-cre) mice with the Cre reporter mice Ai14 to determine td-tomato expression within the brain (Fig. 1c) (Madisen *et al.* 2010). Genomic recombination in NeurK5b-KO was diagnosed by PCR (Fig. 1d). Western blots showed a significant (90%) reduction in Kif5b expression in NeurK5b-KO brains (Fig. 1e and f) compared with control and *Kif5b^{+loxP}*;Tg.Nes-cre mice. Western blots also revealed that Kif5a and Kif5c levels in NeurK5b-KO and in *Kif5b^{+loxP}*;Tg.Nes-cre remain similar to control mice (Fig. 1e and f), suggesting that neuronal *Kif5b* deletion does not induce compensatory expression of other KHC subunits.

We reported that *KLC1* deletion in mice leads to brain malformations and severe transport defects (Falzone *et al.* 2009, 2010). However, neuronal deletion of *Kif5a* and *Kif5c* did not generate brain structural abnormalities (Kanai *et al.* 2000; Xia *et al.* 2003). We analyzed whether neuronal *Kif5b* deletion induced defects in brain architecture. NeurK5b-KO showed no signs of brain developmental defects or survival impairments. To specifically analyze NeurK5b-KO brain structure and morphology we stain nuclei from neural tissue using the thiazine metachromatic dye Toluidine blue. The brain morphology and size of NeurK5b-KO was similar to control at 2 months of age (Fig. 1g). Similar overall morphology and volumes of the brain, cortex, and ventricles were measured in NeurK5b-KO compared with control (Fig. 1h–j); suggesting that *Kif5b* expression is not critical for neuronal development and the acquisition of brain organization.

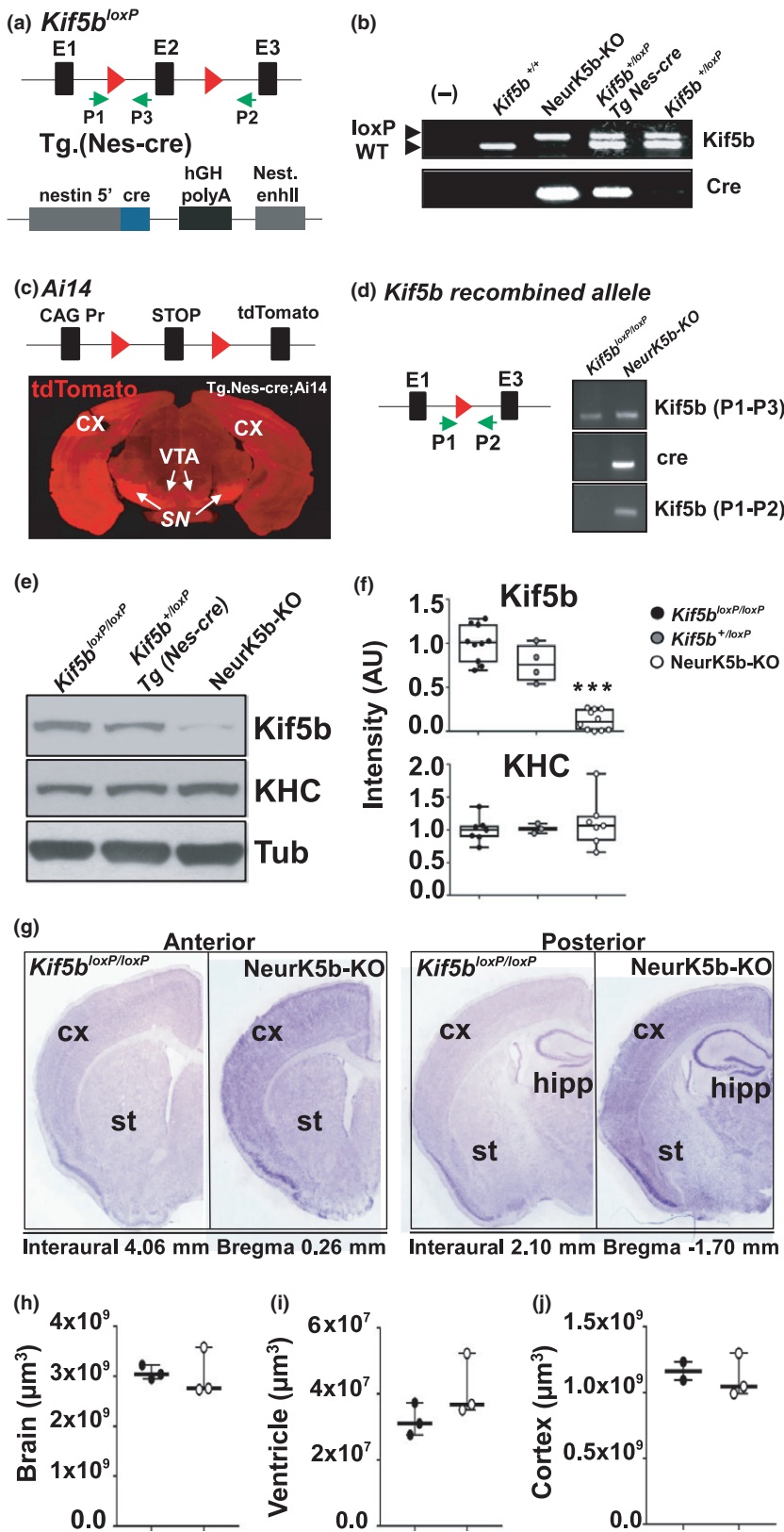


Fig. 1 Neuronal *Kif5b* knockout mice survive and develop a normal brain. (a) Gen map of *Kif5b*^{loxP} (up) and Tg.(Nes-cre) (down) alleles. (b) PCR from *Kif5b*^{+/+}, *Kif5b*^{loxP/loxP}, *NeurK5b-KO* and *Kif5b*^{+/loxP}; Tg.(Nes-cre). *Kif5b* floxed allele amplified a 275 bp. band, wild type a 215 bp. band, and Nes-cre allele a 300 bp. band. Negative control (-). (c) Gen map of *Ai14* allele. Strong promoter (CAG), stop signal and td-tomato are diagramed. Representative image from *Ai14*;Tg.(Nes-cre) brain expressing td-tomato (red). CX: cortex, VTA: ventral tegmental area, and SN: substantia nigra. (d) Recombined *Kif5b*^{loxP} allele and PCR from brain DNA of *Kif5b*^{loxP/loxP} and *NeurK5b-KO* (primers P1-P3, Cre and P1-P2). P1-P2 allowed amplification of recombined alleles. (e) Western blot from brain homogenates extracted from *Kif5b*^{loxP/loxP} (black bar), *Kif5b*^{+/loxP};Tg.Nes-cre (gray bar), and *NeurK5b-KO* (white bar). (f) Western blot quantification for *Kif5b* (one-way ANOVA $F_{(2,21)} = 65.44$, $p < 0.0001$) and kinesin heavy chain (KHC) (one-way ANOVA $F_{(2,14)} = 0.306$, $p < 0.7412$) n : 10 *Kif5b*^{loxP/loxP}, 4 *Kif5b*^{+/loxP};Tg.Nes-cre, and 10 *NeurK5b-KO* brain homogenates. (g) Brain slices from control and *NeurK5b-KO* mice stained with toluidine blue. Anterior (left) and posterior (right) slices indicated following Paxinos atlas coordinates. Cx: Cortex, St: Striatum and Hipp: Hippocampus. (h-j) Quantification of brain (h), ventricles (i), and cortex (j) volumes estimated using the Cavalieri's principle (Student's t -test $t = 0.1641$ $p = 0.1560$ brain, $t = 1.534$ $p = 0.1997$ ventricle, and $t = 0.2443$ $p = 0.8190$ cortex $n = 10$ mice. (** $p < 0.001$).

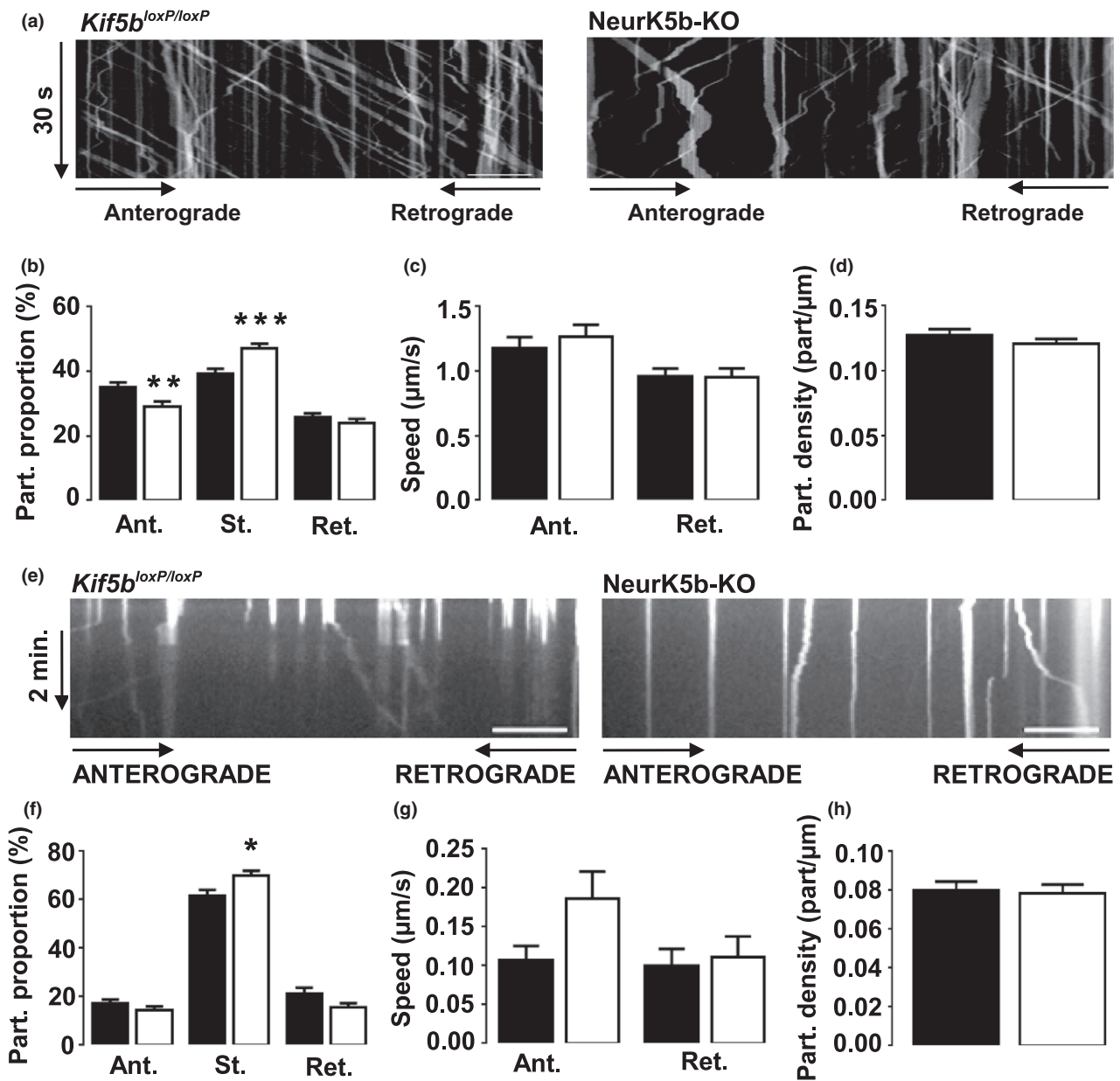


Fig. 2 Impaired amyloid precursor protein (APP) and mitochondria axonal transport in *NeurK5b-KO* neurons. (a) Kymographs of APP-yellow fluorescent protein (YFP) obtained from a 30 s movie in axons from *kif5b^{loxP/loxP}* (left) or *NeurK5b-KO* mice (right). (b) Average proportion of APP-YFP moving in anterograde (ant) or retrograde (ret) direction and those remaining stationary (st) (Student's *t*-test: Ant. $t = 2.695$ $p = 0.0076$, St. $t = 3.454$ $p = 0.0007$ and ret: $t = 0.9551$ $p = 0.3406$). (c) Average speed of APP-YFP vesicles (Student's *t*-test ant: $t = 0.6906$ $p = 0.4909$; ret: $t = 0.08103$ $p = 0.9355$). (d) Average APP-YFP vesicle per micron (Student's *t*-test $t = 1.168$ $p = 0.2440$). $n = 108$ *Kif5b^{loxP/loxP}*, 102 *NeurK5bKO* neurons. (e) Kymographs of

MITO-EGFP from time lapse movies in axons from *kif5b^{loxP/loxP}* (left) or *NeurK5b-KO* mice (right). (f) Average anterograde or retrograde proportion of MITO-EGFP and those remaining stationary (Student's *t*-test ant: $t = 1.286$ $p = 0.2015$; stat: $t = 2.474$ $p = 0.0151$; ret: $t = 1.896$ $p = 0.061$) (g) Average speed of MITO-EGFP (Student's *t*-test ant: $t = 1.921$ $p = 0.0579$; ret: $t = 0.3346$ $p = 0.7388$). (h) Average mitochondria per micron (Student's *t*-test $t = 0.2204$ $p = 0.8260$). $n = 47$ *Kif5b^{loxP/loxP}*, 53 *NeurK5bKO* neurons. Movies of APP-YFP and MITO-EGFP from three independent neuronal cultures using 3–4 pups hippocampi per genotype (Aprox. 12 pups per genotype). * $p < 0.05$, ** $p < 0.01$, *** $p < 0.0001$.

Kif5b deletion induced APP and mitochondria axonal transport defects

To test whether neuronal *kif5b* deletion impairs the axonal transport pathway, we characterized the transport properties

of APP and mitochondria, two distinct cargos that partially depend on *Kif5b* for their movement (Kaether *et al.* 2000; Glater *et al.* 2006). Due to the enrichment and homogeneity of pyramidal neurons obtained from dissected hippocampus

Fig. 3 Hypo-locomotion and discoordination in NeurK5b-KO mice. (a) Timeline followed for *Kif5b*^{loxP/loxP} and NeurK5b-KO at 2 month of age in the open field (Day 1) and rotarod (days 2 and 3). On day 11th the plus maze test was conducted and on day 12th mice were killed for histology, western blot or high pressure liquid chromatography (HPLC) (total timeline A: 27 *Kif5b*^{loxP/loxP} and 21 NeurK5b-KO mice), (b) Total traveled distance by mice in a 30 min open field. (c) Number of movement initiation episodes in the open field. (Student's *t*-test, total distance: $t = 3.79$ $p = 0.0008$; movement initiation: $t = 2.498$ $p = 0.0192$) (d) Distance run in 5-min time period, control black dots and NeurK5b-KO gray dots (two-way ANOVA Bonferroni post hoc test, main effect of genotype $F_{(1,16)} = 9.914$, $p = 0.0062$, main effect of time $F_{(6,96)} = 56.01$, $p < 0.0001$). (e) Proportion of time movement in the center of the open field (Student's *t*-test $t = 2.608$ $p = 0.019$). n : 17 *Kif5b*^{loxP/loxP}, 11 NeurK5b-KO mice. (f) Percentage of entries to closed or open arms (two-way ANOVA, Bonferroni post hoc test, main effect of genotype

$F_{(1,11)} = 3.127$, $p = 0.1047$, main effect of arm $F_{(1,11)} = 32.55$). (g) Percentage of time spent in closed and open arms (two-way ANOVA, Bonferroni post hoc test, main effect of genotype $F_{(1,11)} = 0.3398$, $p = 0.5717$, main effect of arm $F_{(1,11)} = 174.5$). n : 8 *Kif5b*^{loxP/loxP}, 5 NeurK5b-KO mice. (h) Representative mouse footprints in gaiting analysis. (i) Distance between right/left paws (Student's *t*-test right front: $t = 0.4349$ $p = 0.6699$; right back: $t = 1.055$ $p = 0.3081$; left front: $t = 0.2615$ $p = 0.7973$; Left back: $t = 0.1816$ $p = 0.8585$). n : 9 *Kif5b*^{loxP/loxP}, 8 NeurK5b-KO mice. (j) Number of falls from rotarod during each trial, (two-way ANOVA, Bonferroni post hoc, main effect of genotype $F_{(1,27)} = 16.83$, $p = 0.0003$, main effect of trial $F_{(3,81)} = 56.01$, $p < 0.0001$) (k) Maximum time remaining over the rotarod (two-way ANOVA, Bonferroni post hoc, main effect of genotype $F_{(1,27)} = 15.43$, $p = 0.0005$, main effect of trial $F_{(3,81)} = 32.79$, $p < 0.0001$. n : 18 *Kif5b*^{loxP/loxP}, 11 NeurK5b-KO mice. *Kif5b*^{loxP/loxP} black bar and NeurK5b-KO white bar. * $p < 0.05$, ** $p < 0.01$, *** $p < 0.001$.

as opposed to other brain areas we performed primary hippocampal cultures from control and NeurK5b-KO that were transfected with vectors driving fluorescent APP (APP-YFP) or mitochondria (MITO-EGFP) (Fig. 2a and e). *Kif5b* deletion induced specific APP-YFP axonal transport defects with significant decreases in the anterograde proportion of moving vesicles and increases in stationary vesicles (Fig. 2b). No changes were observed in vesicle velocity and density (Fig. 2c and d). In addition, neurons transfected with MITO-EGFP revealed increases in stationary mitochondria in NeurK5b-KO neurons (Fig. 2f). Again, mitochondria velocities and density were similar between controls and NeurK5b-KO (Fig. 2g and h). Thus, deletion of *Kif5b* induced early axonal transport defects of KHC-dependent cargos.

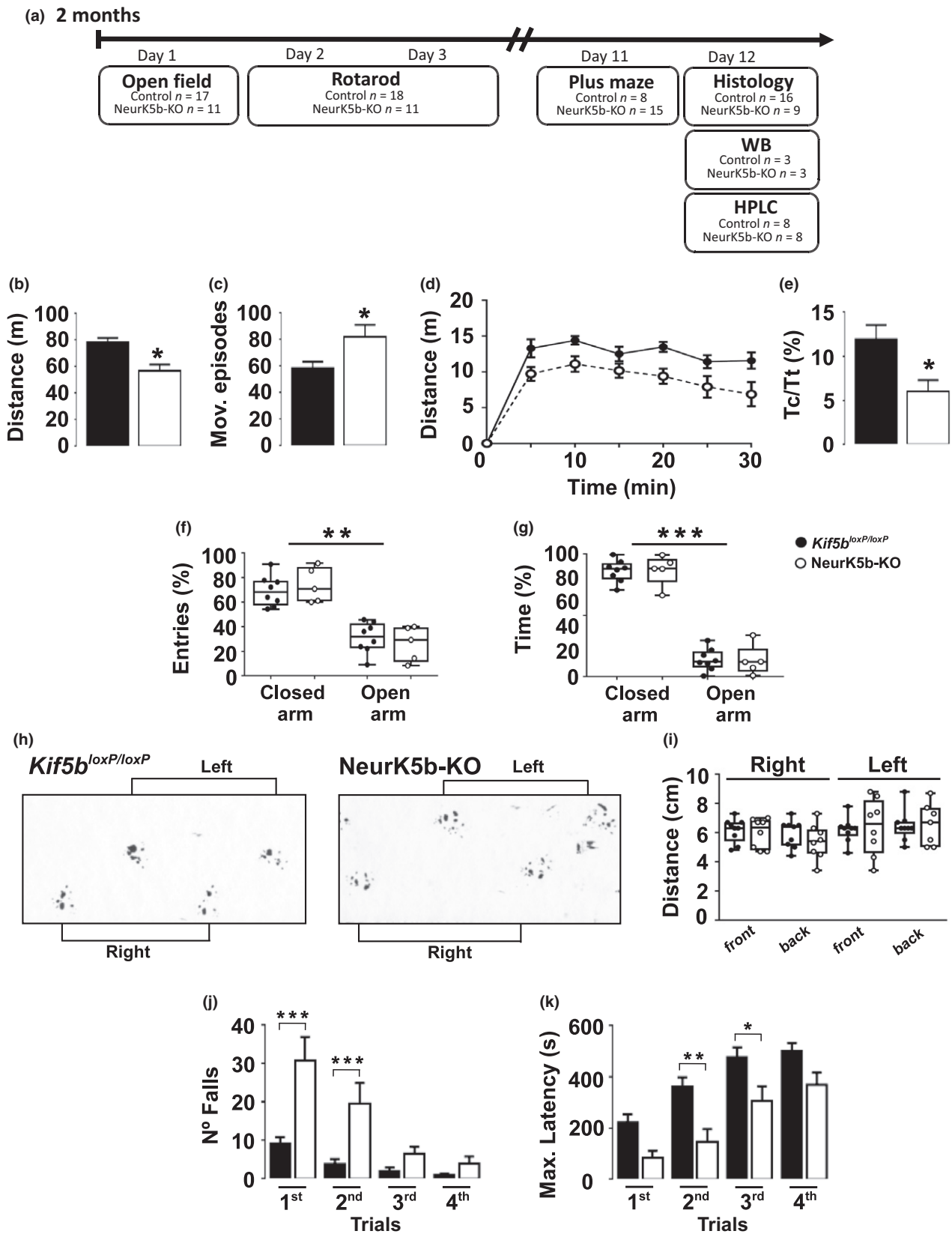
NeurK5b-KO mice show hypo-locomotion and motor coordination deficits

Locomotion is regulated by a complex brain circuitry that involves the motor cortex and the basal ganglia (Gerfen and Surmeier 2011). To test whether locomotor activity is impaired by neuronal *Kif5b* deletion, we performed different behavioral test in NeurK5b-KO mice compared with control (Fig. 3a). Locomotion in the open field was recorded during 30 min and movement responses were analyzed. Interestingly, NeurK5b-KO showed an overall 30% reduction in total traveled distance when compared with control littermates (Fig. 3b), suggesting a hypo-locomotor response. Moreover, NeurK5b-KO showed a 40% increase in the number of ambulatory initiation episodes (Fig. 3c), revealing defects in sustained locomotion performance. To analyze the habituation behavior, the open field experiment was divided in 5-min time lapse and distance measured within each temporal window resulted with similar slope in both genotypes, indicating that hypo-locomotion in NeurK5b-KO was not due to habituation (Fig. 3d). In addition, the events and time of grooming and rearing behavior displayed in the open field by NeurK5b-KO and controls were similar

allowing the discrimination of defects in ambulatory responses but not in stereotypical behavior (Figure S1). In this assay, the proportion of time spent in the center of the open field was reduced in NeurK5b-KO when compared with controls (Fig. 3e), a response that could be related with increased anxiety (Lipkind *et al.* 2004). However, when tested in the elevated plus maze, NeurK5b-KO showed no changes in the proportion of entries and time spent in open arms compared with control (Fig. 3f and g), suggesting that open field results are related to locomotor defects. We then analyzed whether gaiting behavior was impaired in NeurK5b-KO mice by measuring walking steps and left/right paws positioning during locomotion (Fig. 3h). Distance between front and back steps and within right/left legs were normal in NeuroK5b-KO when compared with control (Fig. 3i). In addition, footprint displacement appears normal in NeuroK5b-KO without signs of step discoordination (Fig. 3h and i). However, motor deficits could appear in higher locomotor demanding tasks, such as the rotarod assay. NeurK5b-KO had poor performance on the rotarod with a significant increase in the number of falls (Fig. 3j) and reduced time on the rotating rod compared with controls (Fig. 3k). NeurK5b-KO were able to improve their performance with training over the rotarod, although, they did so at a slower pace (Fig. 3j and k). These results highlight that *Kif5b* expression in neurons is relevant for the process of movement initiation, overall locomotion, and motor coordination.

Impaired DA metabolism in NeurK5b-KO mice

Bradykinesia and movement initiation defects are observed due to low DArgic stimulation within the *striatum* (Fahn 2003). These impairments may appear after significant DArgic neurodegeneration (Shulman *et al.* 2011). To test whether *Kif5b* deletion induce cell loss, we quantified the number of DArgic neurons in the *SN* and ventral tegmental area (VTA). Serial coronal brain sections from NeurK5b-KO and control mice were stained against TH



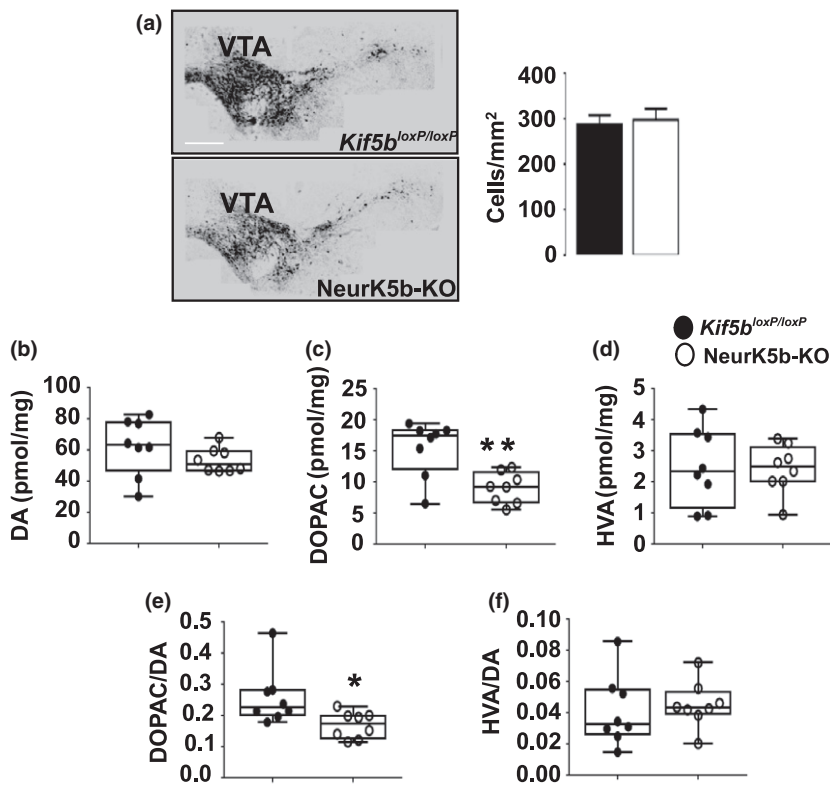


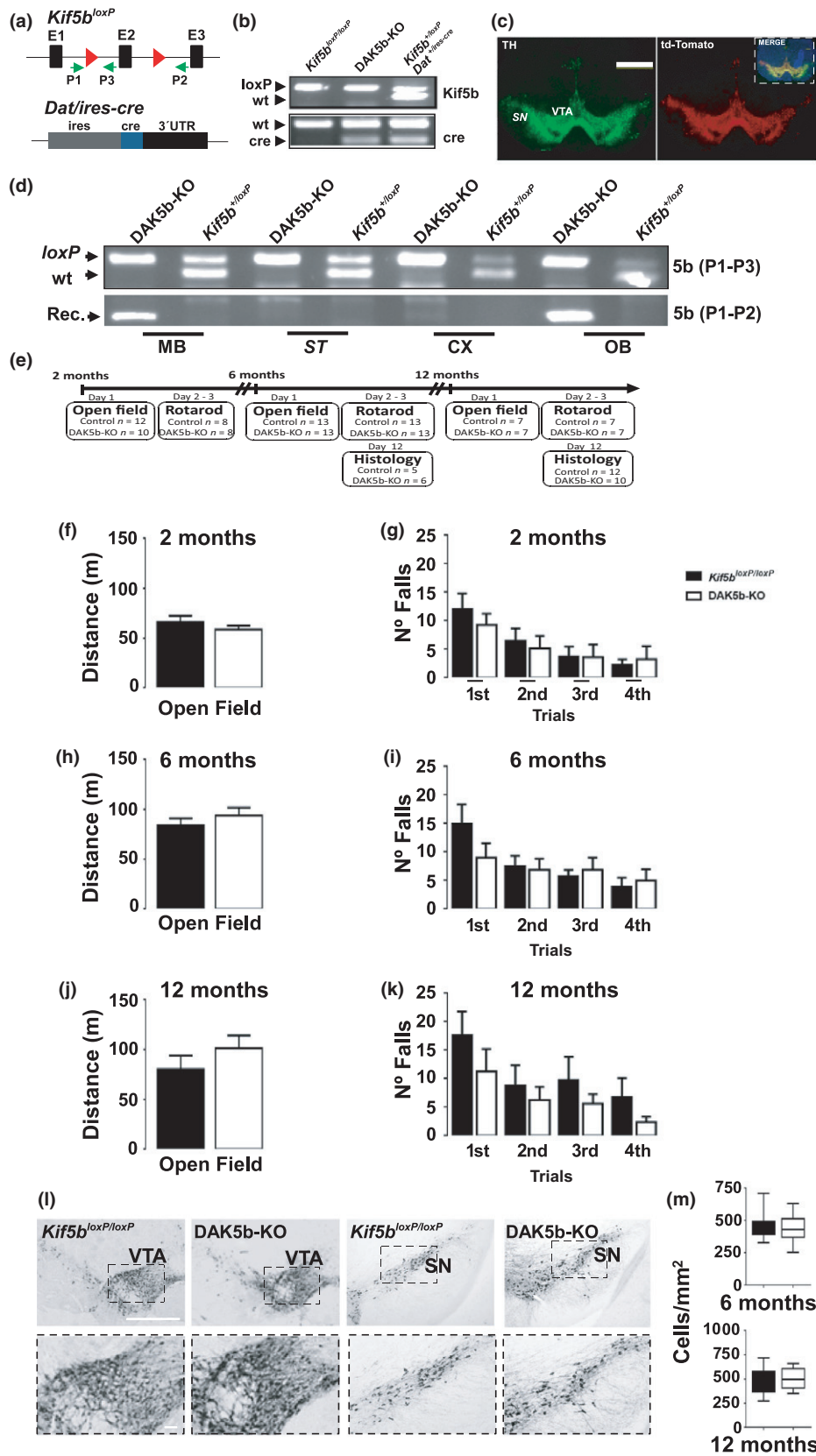
Fig. 4 DA metabolism impairments in *NeurK5b-KO* mice. (a) Tyrosine hydroxylase immunohistochemistry in brain slices from *Kif5b^{loxP/loxP}* and *NeurK5b-KO* (Student's *t*-test $t = 0.2705$ $p = 0.79$). n : 16 *Kif5b^{loxP/loxP}*, 9 *NeurK5b-KO* mice. (b–f) Concentration of total DA (b), DOPAC (c), HVA (d), DOPAC/DA (e) and HVA/DA (f) measured by high pressure liquid chromatography in pico-mol per milligram of total proteins (pmol/mg). (Student's *t*-test DA $t = 1.233$ $p = 0.2377$, DOPAC: $t = 3.564$ $p = 0.031$, HVA: t -test $t = 0.09878$ $p = 0.9227$, DOPAC/DA: $t = 2.513$ $p = 0.0248$; and HVA/DA: $t = 0.4253$ $p = 0.6771$). *Kif5b^{loxP/loxP}* black dots, *NeurK5b-KO* white dots. * $p < 0.05$, ** $p < 0.01$.

(Fig. 4a). TH-positive cells were quantified revealing similar density of DA neurons in *NeurK5b-KO* and control (Fig. 4b). To test whether *Kif5b* deletion impairs DA metabolism in the *striatum*, we analyzed by high pressure liquid chromatography striatal DA concentration and its intracellular and extracellular metabolites, DOPAC and HVA, respectively (Fig. 4c–g). We found similar DA concentrations in the *striatum* of *NeurK5b-KO* and control (Fig. 4c), suggesting that *Kif5b* deletion had no effect on the steady state levels of DA within DArg terminals.

However, DOPAC was significantly decreased in *NeurK5b-KO* (Fig. 4d). In addition, DOPAC/DA ratio was lower in *NeurK5b-KO* mice, indicating a reduction in the DA intracellular degradation rate (Fig. 4f). Noteworthy, HVA striatal concentration was similar in both genotypes (Fig. 4e), showing no differences in HVA/DA ratio and suggesting that *NeurK5b-KO* were able to sustain similar basal levels of DA release in resting conditions (Fig. 4g). Together, these results suggest that reduced rates of DA synthesis and/or degradation within pre-synaptic striatal

Fig. 5 Normal locomotion in *DAK5b-KO* mice. (a) Gen map of *Kif5b^{loxP}* (up) and *Dat^{+/ires-cre}* alleles (down). (b) PCR from *Kif5b^{loxP/loxP}*, *DAK5b-KO* and *Kif5b^{+/loxP}; dat^{+/ires-cre}*. *Kif5b* floxed allele amplified a 275 bp. band, wild type a 215 bp. band (up). Cre in heterozygosis amplified two bands at 264 bp. and 152 bp. (down). (c) Tyrosine hydroxylase (TH) immunofluorescence (green) from *Ai14;Dat^{+/ires-cre}* expressing td-tomato (red) in *Substantia nigra* (SN) and ventral tegmental area (VTA). Hoechst staining to observed nuclei (blue). Scale bar: 1 mm (d) PCR from DNA extracted from midbrain (MB), *striatum* (ST), cortex (CX) and olfactory bulb (OB) in *Kif5b^{+/loxP}* and *DAK5b-KO*. Amplification was observed from WT or *loxP* alleles using P1–P3 primers (upper) and after recombination using P1–P2 primers in DA neurons (lower) from *DAK5b-KO* at MB and OB. (e) Experimental timeline followed for *Kif5b^{loxP/loxP}* and *DAK5b-KO* mice at 2, 6, and 12 months of age in the open field (Day 1) and rotarod (days 2 and 3). On day 12-, 6-, or 12-month-old mice were killed for histology (total: 17 *Kif5b^{loxP/loxP}* and 18 *DAK5b-KO* mice). (f, h, j) Total traveled distance in a 30-min open field at 2-, 6-, and 12-month-old

mice [Student's *t*-test (f): $t = 1.11$ $p = 0.2801$, n : control 12, *DAK5b-KO* 10 mice; (h): $t = 1.11$ $p = 0.2801$, n : 13 *Kif5b^{loxP/loxP}*, 13 *DAK5b-KO* mice, and (j): $t = 0.9509$ $p = 0.3511$, n : 7 *Kif5b^{loxP/loxP}*, 7 *DAK5b-KO* mice]. (g, i, k) Number of falls from the rotarod at 2-, 6-, and 12-month-old mice [two-way ANOVA, (g) main effect of genotype $F_{(1,14)} = 0.09177$, $p = 0.7664$, main effect of trial $F_{(3,42)} = 22.45$, $p < 0.0001$ n : 8 *Kif5b^{loxP/loxP}*, 8 *DAK5b-KO* mice; (i) main effect of genotype $F_{(1,24)} = 0.1897$, $p = 0.6671$, main effect of trial $F_{(3,72)} = 7.502$, $p = 0.0002$ n : 13 *Kif5b^{loxP/loxP}*, 13 *DAK5b-KO* mice; (k) main effect of genotype $F_{(1,12)} = 1.166$, $p = 0.3014$, main effect of trial $F_{(3,36)} = 9.936$, $p < 0.0001$ n : 7 *Kif5b^{loxP/loxP}*, 7 *DAK5b-KO* mice. *Kif5b^{loxP/loxP}*: black bar, *DAK5b-KO*: white bar. (l) TH immunohistochemistry from 12-month-old *Kif5b^{loxP/loxP}* and *DAK5b-KO*. Scale 1 mm (up) and 50 μ m (down). (m) Quantification of TH⁺ cell density from 6 (n : 5 *Kif5b^{loxP/loxP}*, 6 *DAK5b-KO*) and 12 months-old mice (n : 12 *Kif5b^{loxP/loxP}*, 10 *DAK5b-KO*) (Student's *t*-test 6 months: $t = 0.3545$ $p = 0.3627$, 12 months $t = 0.2089$ $p = 0.8354$).



terminals may lead to deficits in locomotion and motor coordination in NeurK5b-KO mice.

Normal locomotion observed after conditional deletion of *Kif5b* only in dopaminergic neurons

To test whether locomotor defects are induced by pre-synaptic impairments in DArgic neurons we generated a strain carrying *Kif5b* null alleles exclusively in DArgic neurons. *Kif5b^{loxP/loxP}* mice were crossed with transgenic mice expressing Cre under the control of an Internal Ribosome Entry Site (IRES) within the DA transporter (*Dat*) gene (*Dat^{+ires-cre}*) (Bäckman *et al.* 2006) (Fig. 5a and b). The specific activity of cre in DArgic neurons in *Dat^{+ires-cre}* was tested by crossing it with the Ai14 reporter mice and analyzing the expression of td-Tomato counterstained against TH in VTA and SN (Fig. 5c). The conditional genomic recombination of *Kif5b* gene in *Kif5b^{loxP/loxP};Dat^{+ires-cre}* (from now on: DAK5b-KO) was confirmed by PCR revealing amplification only from midbrain and olfactory bulb DNA where DArgic neurons are located, but not from striatum and cortex, or from control *Kif5b^{+loxP}* without Cre (Fig. 5d). The experimental setting followed to analyzed DAK5b-KO mice was performed at 2, 6, and 12 months of age (Fig. 5e). When evaluated in the open field similar locomotor responses were observed in DAK5b-KO compared with control mice at 2 months of age (Fig. 5f). In addition, 6 and 12 months-old DAK5b-KO showed normal locomotion (Fig. 5h and j). Moreover, DAK5b-KO mice displayed normal motor coordination behavior when tested in the rotarod showing similar numbers of falls and time on the rod at 2, 6, and 12 months of age compared with control (Fig. 5g, i and k; Figure S2). DArgic neuron survival was not compromised in DAK5b-KO, displaying similar density of TH-positive neurons in the VTA and SN when compared with control mice at 6 and 12 months of age (Fig. 5l and m). Together, these results suggest that conditional deletion of *Kif5b* from pre-synaptic DArgic neurons is not sufficient to induce locomotor defects like those observed after conditional deletion of *Kif5b* throughout the brain.

Dopamine receptor mediated locomotor defects in NeurK5b-KO mice

To test whether locomotor impairments observed in NeurK5b-KO were caused by post-synaptic defects in the striatum, we induced DA release using amphetamine (7.5 mg/kg, i.p.) and measured locomotion (Sharp *et al.* 1987). Mice placed in the open field after 15 min of a single amphetamine injection revealed a significant increase in total traveled distance in NeurK5b-KO and control mice compared with PBS injection as control (Fig. 6a and b). Amphetamine induced a significant increase in total traveled distance in the open field in NeurK5b-KO and control mice (Fig. 6a). On the other hand, mice of both genotypes receiving amphetamine showed reduced movement initiation episodes, in accordance with the facilitation of

sustained locomotion (Fig. 6b). To gain further insight about the mechanisms that induce locomotor disorders in NeurK5b-KO, we studied the effects of the D1R antagonist SCH23390 in the open field. SCH 23390 (0.25 mg/kg) induced a significant decrease in total traveled distance and an overall reduction in the number of movement initiation episodes in control and NeurK5b-KO (Fig. 6c and d). D2R contribution to movement was analyzed by the administration of the D2R agonist quinpirole (0.05 mg/kg) which induced a significant reduction in total traveled distance in both genotypes, although did not change the number of movement initiation episodes (Fig. 6c and d). The effect of SCH 23390 or quinpirole was then tested in amphetamine-treated mice. Pre-treatment with SCH 23390 reduced the total traveled distance compared to amphetamine-induced locomotion in both genotypes (Fig. 6e). However, D1R antagonist significantly increased the number of movement initiation episodes in control and NeurK5b-KO (Fig. 6f). Contrarily, while quinpirole did not modify the traveled distance induced by amphetamine in both genotypes (Fig. 6e); it significantly increased the number of amphetamine-induced movement initiation episodes in control mice. However, no effect was observed in the number of initiation episodes in NeurK5b-KO, highlighting a significant difference in D2R-mediated locomotion between both genotypes (Fig. 6f). These results suggest that modulation of movement initiation responses depends on D2R activation and that *Kif5b* deletion may impair D2R-mediated signaling.

Impaired subcellular distribution of D2R in NeurK5b-KO

Selective differences were observed in D2R activity. We, therefore, tested whether the expression and localization of DA receptors was impaired in NeurK5b-KO. Striatal *Drd1* and *Drd2* expression levels determined by quantitative RT-PCR were similar in mice of both genotypes (Fig. 7a and b), indicating that DA receptors expression was not impaired by *Kif5b* deletion. We then tested whether protein levels or localization of the D2R might be altered. The striatum from control and NeurK5b-KO were extracted and fractionated to analyze D2R protein levels and its subcellular distribution (Fig. 7c, Figure S3). Similar amounts of D2R protein were observed in striatum homogenate fraction from control and NeurK5b-KO when normalized to tubulin, consistent with normal levels of mRNA expression (Fig. 7c and d). The levels of NMDA receptor, a protein that does not depend on Kinesin-1 for its membrane presentation and recycling (Setou *et al.* 2000), were used as control for synaptic plasma membrane fraction (LP1) enrichment. (Fig. 7c and d). Quantification of D2R normalized to NMDAR revealed enrichment in striatal LP1 compared with homogenate fraction in control mice (Figure S3). However, a significant reduction in D2R levels in synaptic plasma membrane fraction was observed in NeurK5b-KO when compared with controls (Fig. 7d, Figure S3). These experiments suggest that deletion of *Kif5b* from striatal neurons does not change total

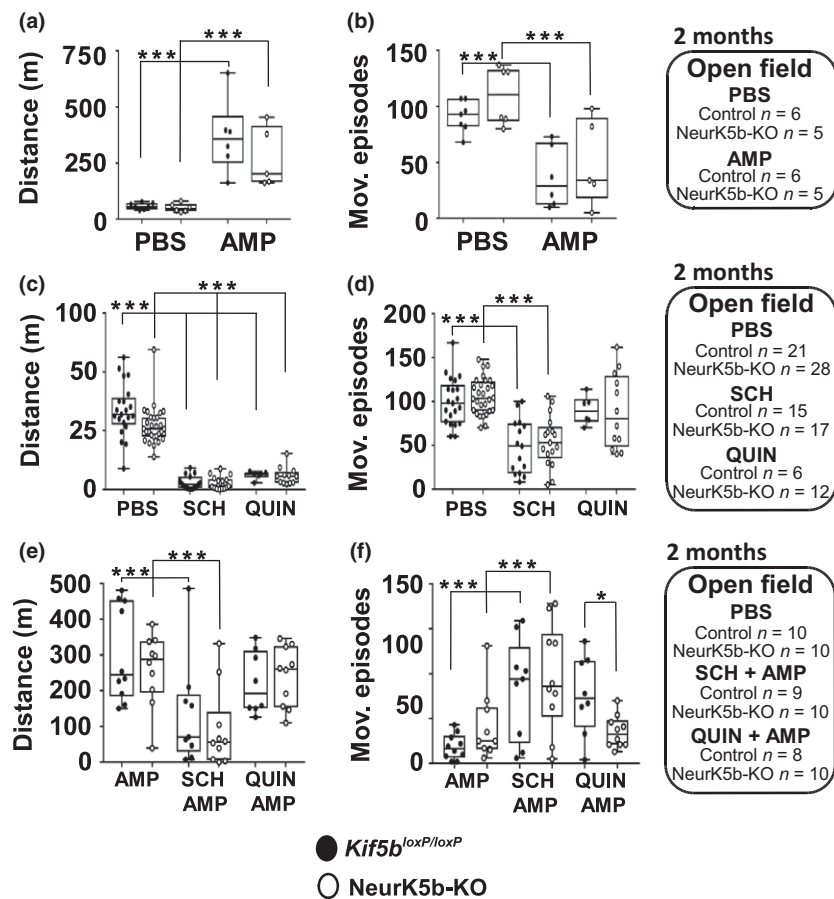


Fig. 6 Impaired dopamine D2 receptor (D2R) dependent movement initiation in NeurK5b-KO. (a) Total traveled distance and (b) movement initiation episodes in the open field for mice injected with PBS or amphetamine (AMP). Two-way ANOVA Bonferroni post hoc test, (a): main effect of genotype $F_{(1,20)} = 1.481$, $p = 0.2377$; main effect of drug $F_{(1,20)} = 40.05$, $***p < 0.0001$, (b): main effect of genotype $F_{(1,20)} = 2.13$, $p = 0.16$; main effect of drug $F_{(1,20)} = 27.03$, $p < 0.0001$. $n: 6 Kif5b^{loxP/loxP}$ PBS, 5 NeurK5b-KO PBS, 6 $Kif5b^{loxP/loxP}$ AMP, 5 NeurK5b-KO AMP mice. (c) Total traveled distance and (d) movement initiation episodes in open field for PBS, SCH 23390 (SCH) or Quinpirole (QUIN) injected mice. Two-way ANOVA Bonferroni post hoc test, (c): main effect of genotype $F_{(1,93)} = 1.99$, $p = 0.1617$; main effect of drug $F_{(2,93)} = 165.8$, $p < 0.0001$; (d): main effect of genotype $F_{(1,93)} = 0.3389$, $p = 0.5619$; main effect of drug $F_{(2,93)} = 32.11$,

$p < 0.0001$. $n: 21 Kif5b^{loxP/loxP}$ PBS, 28 NeurK5b-KO PBS, 15 $Kif5b^{loxP/loxP}$ SCH, 17 NeurK5b-KO SCH, 6 $Kif5b^{loxP/loxP}$ QUIN, 12 NeurK5b-KO QUIN mice. (e) Total traveled distance and (f) movement initiation episodes in the open field for AMP, SCH + AMP, or QUIN + AMP injected mice. Two-way ANOVA Bonferroni post hoc test, (e): main effect of genotype $F_{(1,51)} = 0.05801$, $p = 0.4498$; main effect of drug $F_{(2,51)} = 10.98$, $p = 0.0001$; (f): main effect of genotype $F_{(1,51)} = 0.05244$, $p = 0.8198$; main effect of drug $F_{(2,51)} = 10.34$, $p = 0.0002$. n AMP: 10 $Kif5b^{loxP/loxP}$, 10 NeurK5b-KO. n SCH + AMP: 9 $Kif5b^{loxP/loxP}$, 10 NeurK5b-KO. n QUIN + AMP: 8 $Kif5b^{loxP/loxP}$, 10 NeurK5b-KO mice. Boxes correspond to number of mice tested in the open field at 2 months of age from a naïve cohort. $Kif5b^{loxP/loxP}$ black bar, NeurK5b-KO white bar. * $p < 0.05$, *** $p < 0.001$.

D2R protein levels, but impairs D2R stabilization at the plasma membrane. Together, these results reveal the participation of Kif5b in the presentation and recycling of striatal plasma membrane D2R that control movement initiation, locomotion, and motor coordination.

Discussion

Intracellular dynamics support the distribution and presentation of proteins necessary for neurotransmission. The intricate neuronal connectivity in the basal ganglia depends on

intracellular dynamics to modulate the behavioral response of locomotion. Therefore, understanding the contribution of motor proteins to neuronal function is relevant to comprehend the system and unravel the locomotor defects associated with disorders of movement.

The process of movement initiation and motor coordination relies on DA release from the *substantia nigra pars compacta* to striatal MSN expressing DA receptors (Bolam, 2000; Gerfen and Surmeier 2011). The coordinated stimulation of D1R and D2R allow the fine tune regulation required for movement (Gerfen *et al.* 1990; Mink 2003), and

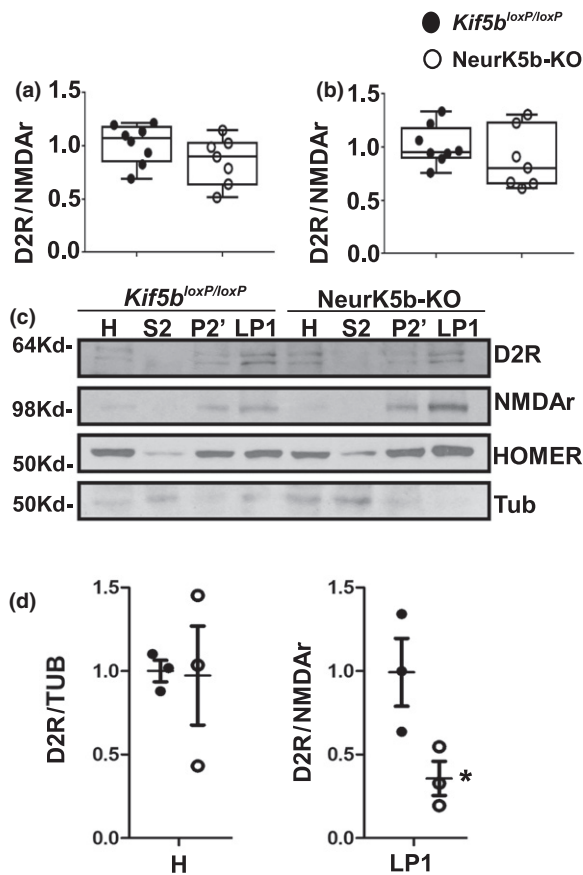


Fig. 7 NeurK5b-KO display lower levels of membrane dopamine D2 receptor (D2R) in *striatum*. (a) *Drd1*mRNA and (b) *Drd2*mRNA quantification by RT-PCR from cDNA prepared from mice *striatum* mRNA. (Student's *t*-test $t = 1.522$ $p = 0.1520$). *n*: 8 *Kif5b^{loxP/loxP}*, 7 NeurK5b-KO *striata*. (c) Western blot from fractions obtained after differential centrifugation. Homogenate (H), supernatant (S2), crude synaptosomes (P2'), and synaptic plasma membrane (LP1) obtained after centrifugations from *Kif5b^{loxP/loxP}* and NeurK5b-KO *striata*. (d) Quantification of D2R distribution normalized to tubulin in homogenate (H) and to NMDAR in plasma membrane (LP1) fractions from *Kif5b^{loxP/loxP}* and NeurK5b-KO (Student's *t*-test $t = 2790$ $p = 0.0493$). *n*: 3 *Kif5b^{loxP/loxP}*, 3 NeurK5b-KO. *Kif5b^{loxP/loxP}* black, NeurK5b-KO white. * $p < 0.05$.

impairments in MSN activity leads to locomotor defects (Starr and Starr 1986; Baik *et al.* 1995; Kelly *et al.* 1998; Usiello *et al.* 2000). We generated conditional deletions of *kif5b* to study the locomotor response in mice. NeurK5b-KO display normal size and growth; however, *Kif5b* deletion from neurons induces early axonal transport impairments of APP and mitochondria. While mild defects were observed in overall transport of these cargos, impairments may arise in the long term as it is observed when behavior was analyzed in NeurK5b-KO. Interestingly, significant hypo-locomotion was observed at 2 month of age in NeurK5b-KO, including lower travelled distance and increased movement initiation

attempts. These results suggest selective impairments associated with the circuitry that controls movement. The neuronal deletion of other KHC subunit, such as KIF5a, severely compromised mice survival and the main phenotype observed involved epileptic behavior but no locomotor defects (Xia *et al.* 2003; Nakajima *et al.* 2012). Interestingly, neither peripheral neuronal defects, nor epileptic behavior were observed in NeurK5b-KO compared with conditional *Kif5a* deletion, suggesting differential roles for distinct KHC subunits of kinesin-1. NeurK5b-KO showed severe defects in motor coordination when tested in a demanding task, such as the rotarod. Similar motor coordination impairments were observed in D1R and D2R knockout mice (Nakamura *et al.* 2014). Moreover, mice treated with MPTP, a selective DArgic neurodegenerative agent, also showed motor coordination impairments (Ayton *et al.* 2013), however, DA neuron degeneration was not observed in NeurK5b-KO. Our results suggest that activity of the nigrostriatal system that control locomotion is impaired in NeurK5b-KO.

DA metabolism and its extracellular release depends on axonal transport of various enzymes and organelles (Matsuda *et al.* 2009). NeurK5b-KO display specific defects in DA metabolism observed by reduced DOPAC, without changes in DA or HVA levels, suggesting that DA availability and release in steady-state conditions were similar in both genotypes. Since DA synthesis is controlled by TH feedback inhibition (Meiser *et al.* 2013), a reduced intracellular degradation did not lead to increased DA amounts. A similar phenotype was described in monoamine oxidase (MAO)-A KO mice with almost similar DA levels but significant reductions in DOPAC (Cases *et al.* 1995). MAO, in charge of intracellular conversion of DA to DOPAC, is located at the mitochondrial external membrane (Westlund *et al.* 1993). Interestingly, we showed that neurons with *Kif5b* deletion in culture display significant increases in stationary mitochondria suggesting less dynamic organelles reaching distal synapses. Therefore, a reduced number of mitochondria in striatal innervations due to transport defects may lead to diminished presence of MAO and DOPAC. It is relevant to stress that DAergic neurodegeneration induced by MPP⁺ involves the destabilization of microtubules and specific defects in mitochondria transport (Cartelli *et al.* 2010; Kim-Han *et al.* 2011; Dukes *et al.* 2016;). Thus, a limited metabolic load in extensive polarized projections have been proposed to contribute to the selective vulnerability of DA neurons (Bolam and Pissadaki 2012; Pozo Devoto and Falzone 2017). Under this condition, it is possible that compromised locomotion associated with abnormal DA availability under demanding tasks appear in challenged coordinated locomotion, or exploring a novel environment (Lisman and Grace 2005; Kumakura *et al.* 2010). Interestingly, selective deletion of *kif5b* from DArgic neurons in DAK5b-KO did not induce hypo-locomotion or motor coordination impairments, demonstrating that absence of

kif5b only in those neurons is not sufficient to generate locomotor defects. These results suggest that pre-synaptic defects on DA metabolism in NeurK5b-KO might be a consequence of impaired striato-nigral regulation of DArgic neuronal activity.

The stimulation of DA release by amphetamine-induced hyper-locomotion and reduced the attempts for movement initiation in control and NeurK5b-KO mice. DArgic receptor stimulation at the post-synapse is fundamental for the activity of the direct and indirect pathway during locomotion (Cui *et al.* 2014). Even, cortical neurons that release glutamate to MSN and express D2R can be modulated by DA (Bamford *et al.* 2004). D1R and D2R are actively transported within neurons (van Der Kooy *et al.* 1986; Aiso *et al.* 1987), and their presentation at the membrane requires the function of motor proteins for a regulated endocytosis and recycling process, highlighting the relevance of motor proteins for intracellular dynamics and neuronal function (van Der Kooy *et al.* 1986; Aiso *et al.* 1987; Migheli *et al.* 2013; Rassa *et al.* 2017). The increase in movement initiation episodes associated with hypo-locomotion in NeurK5b-KO is proposed as abnormal attempts to achieve proper locomotion. These locomotor defects depend on D2R stimulation since quinpirole regulate this phenotype in amphetamine-induced control mice. However, NeurK5b-KO were insensitive to D2R-mediated movement initiation phenotype modulated by quinpirole, which has a biphasic effect on mice movement inducing hypo-locomotion at low doses (Luque-Rojas *et al.* 2012). The pre-synaptic deletion of D2Rs lead to increased locomotor activity and mice resulted insensitive to hypo-locomotion induced by quinpirole (Bello *et al.* 2012). Contrarily, post-synaptic D2R deletion leads to hypo-locomotion but this response can be further reduced by low doses of quinpirole (Anzalone *et al.* 2012). These results stress the role of D2R in movement regulation suggesting that NeurK5b-KO impairments in locomotion might be due to post-synaptic defects in D2R. Noteworthy, constitutive D2R deletion in mice induced hypo-locomotion (Kelly *et al.* 1998), while D1R-KO showed hyperactivity (Xu *et al.* 1994) or no evident locomotor impairments (Drago *et al.* 1994). In agreement with our results, the stimulation of the indirect pathway using optogenetics specifically reduced the number of movement initiation episodes (Kravitz *et al.* 2010). Therefore, in NeurK5b-KO, functional defects of post-synaptic D2R could mediate hypo-locomotion, increased number of movement episodes, impaired DA metabolism, and lack of sensitivity to quinpirole under stimulation with amphetamine. However, our experiments did not rule out the possibility that locomotor impairments in NeurK5b-KO might be originated by transport defects in cortical neurons that project toward the *striatum*. Moreover, since glutamatergic stimulation in the *striatum* is regulated by DA in a complex synaptic arrangement with D2R present both in

MSN dendrites and in cortical axons (Wang and Pickel 2002; Bamford *et al.* 2004).

Different PD models suggest that intracellular defects in the recycling of DA receptors could lead to impaired neuronal function and locomotion (Migheli *et al.* 2013; Rassa *et al.* 2017). In fact, subcellular fractionation from NeurK5b-KO *striatum* determined a decrease in D2R levels in synaptic plasma membranes compared with control, suggesting that Kif5b is important for the presentation or maintenance of D2R at the cell surface. The desensitization process of D2R occur through endocytosis upon DA stimulation, a mechanism that depends on clathrin- β -arrestin complexes (Kim *et al.* 2001). Studies in MSN cultures determined that D2R are internalized by two pathways (Li *et al.* 2012): agonist-independent endocytosis through Rab4-sensitive fast recycling pathway, and agonist-dependent endocytosis through Rab11 slow recycling pathway. Kif5b interacts with both Rab4 and Rab11 through protein complexes (Schmidt *et al.* 2009), so D2R recycling mechanisms could be impaired in NeurK5b-KO. Despite the lack of motor phenotypes in DAK5b-KO and the fact that post-synaptic D2R deletion induced hypo-locomotion (Anzalone *et al.* 2012), it is possible that D2R in MSN are abnormally distributed in NeurK5b-KO, suggesting an important role for Kif5b in D2R distribution. Together, these data establish a causal role for the stimulation of post-synaptic D2R in the indirect pathway that regulates ambulatory initiation episodes, a relevant step in overall locomotion processes. These results are relevant for understanding how motor protein defects contribute to the induction of locomotor impairments that can be linked to the clinical manifestations found in neurodegenerative disorders of movement.

Acknowledgments and conflict of interest disclosure

We kindly thank Dr. Nancy Jenkins for providing *kif5b^{loxP/loxP}* mice. T.L.F. acknowledges support from CONICET, Universidad de Buenos Aires, and the Argentinean Science Ministry. V.M.P.D., M.A., M.G.O., T.M.S., and L.E.C. acknowledge support from CONICET fellowships. This work was supported by grants from MINCyT (PICT 2011–2027; 2013-0402, T.L.F.); the Alzheimer Association (NIRG10-172840, T.L.F.); and Universidad de Buenos Aires (UBACyT 2011/2014, T.L.F.). The authors declare no conflict of interest.

All experiments were conducted in compliance with the ARRIVE guidelines.

Open science badges

This article has received a badge for *Open Materials* because it provided all relevant information to reproduce the study in the manuscript. The complete Open Science Disclosure form for this article can be found at the end of the article. More information about the Open Practices

badges can be found at <https://cos.io/our-services/open-science-badges/>.

Supporting information

Additional supporting information may be found online in the Supporting Information section at the end of the article.

Figure S1. NeurK5b-KO mice display normal stereotypical behavior in the open field.

Figure S2. Normal rotarod performance in DAK5b-KO mice.

Figure S3. Three sets of western blots generated from fractions obtained after differential centrifugation.

References

- Aiso M., Potter W. Z. and Saavedra J. M. (1987) Axonal transport of dopamine D1 receptors in the rat brain. *Brain Res.* **426**, 392–396.
- Anzalone A., Lizardi-Ortiz J. E., Ramos M. *et al.* (2012) Dual control of dopamine synthesis and release by presynaptic and postsynaptic dopamine D2 receptors. *J. Neurosci.* **32**, 9023–9034.
- Ayton S., George J. L., Adlard P. A., Bush A. I., Cherny R. A. and Finkelstein D. I. (2013) The effect of dopamine on MPTP-induced rotarod disability. *Neurosci. Lett.* **543**, 105–109.
- Bäckman C. M., Malik N., Zhang Y., Shan L., Grinberg A., Hoffer B. J. and Westphal H. T. A. (2006) Characterization of a mouse strain expressing Cre recombinase from the 3' untranslated region of the dopamine transporter locus. *Genesis* **390**, 383–390.
- Baik J., Picetti R., Saiardi A., Thiriet G., Dierich A., Depaulis A., Le Meur M. and Borrelli E. (1995) Parkinsonian-like locomotor impairment in mice lacking dopamine D2R receptors. *Nature* **377**, 424–428.
- Bamford N. S., Robinson S., Palmiter R., Joyce J., Moore C. and Meshul C. (2004) Dopamine modulates release from corticostriatal terminals. *J. Neurosci.* **24**, 9541–9552.
- Bello E. P., Mateo Y., Gelman D., Noaín D., Shin J., Low M. J., Alvarez V. A., Lovinger D. M. and Rubinstein M. (2012) Cocaine supersensitivity and enhanced motivation for reward in mice lacking dopamine D2R autoreceptors. *Nat. Neurosci.* **14**, 1033–1038.
- Bolam J. P., Hanley J. J., Booth P. A. and Bevan M. D. (2000) Synaptic organisation of the basal ganglia. *J. Anat.* **196**(Pt 4), 527–542.
- Bolam J. P. and Pissadaki E. K. (2012) Living on the edge with too many mouths to feed: why dopamine neurons die. *Mov. Disord.* **12**, 1478–1483.
- Braak H. and Braak E. (1990) Cognitive impairment in Parkinson's disease: amyloid plaques, neurofibrillary tangles, and neurophil threads in the cerebral cortex. *Neural Transm.* **2**, 45–57.
- Cartelli D., Ronchi C., Maggioni M. G., Rodighiero S., Giavini E. and Cappelletti G. (2010) Microtubule dysfunction precedes transport impairment and mitochondria damage in MPP⁺-induced neurodegeneration. *J. Neurochem.* **115**(1), 247–258.
- Cases O., Seif I., Grimsby J., Chen K., Pourmin S., Muller U., Aguet M., Babinet C., Shih J. C. (1995) Aggressive behavior and altered amounts of brain serotonin and norepinephrine in mice lacking MAOA. *Science* **268**, 1763–1766.
- Chu Y., Morfini G. A., Langhamer L. B., He Y., Brady S. T. and Kordower J. H. (2012) Alterations in axonal transport motor proteins in sporadic and experimental Parkinson's disease. *Brain* **135**, 2058–2073.
- Cui J., Wang Z., Cheng Q., Lin R., Zhang X., Leung P. S., Copeland N. G., Jenkins N. A., Yao K. and Huang J. (2011) Targeted inactivation of kinesin-1 in pancreatic β -cells in vivo leads to insulin secretory deficiency. *Diabetes* **60**, 320–330.
- Cui G., Jun S. B., Jin X., Pham M. D., Vogel S. S., Lovinger D. M. and Costa R. M. (2014) Concurrent activation of striatal direct and indirect pathways during action initiation. *Nature* **494**, 238–242.
- De Vos K. J., Grierson A. J., Ackerley S. and Miller C. C. J. (2008) Role of axonal transport in neurodegenerative diseases. *Annu. Rev. Neurosci.* **31**, 151–173.
- Deboer S. R., You Y., Szodorai A., Kaminska A., Nwabuisi E., Wang B., Estrada-hernandez T., Kins S., Scott T. and Morfini G. (2009) Conventional Kinesin holoenzymes are composed of heavy and light chain homodimers. *Biochemistry* **47**, 4535–4543.
- van Der Kooy D., Weinreich P. and Nagy J. I. (1986) Dopamine and opiate receptors: localization in the striatum and evidence for their axoplasmic transport in the nigrostriatal and striatonigral pathways. *Neuroscience* **19**, 139–146.
- Drago J., Gerfen C. R., Lachowicz J. E. *et al.* (1994) Altered striatal function in a mutant mouse lacking D1A dopamine receptors. *Proc. Natl Acad. Sci. USA* **91**, 12564–12568.
- Dukes A. A., Bai Q., Van Laar V. S. *et al.* (2016) Live imaging of mitochondrial dynamics in CNS dopaminergic neurons in vivo demonstrates early reversal of mitochondrial transport following MPP(+) exposure. *Neurobiol. Dis.* **95**, 238–249.
- Fahn S. (2003) Description of Parkinson's disease as a clinical syndrome. *Ann. N. Y. Acad. Sci.* **991**, 1–14.
- Falzone T. L. and Stokin G. B. (2012) Imaging amyloid precursor protein in vivo: an axonal transport assay, in *Neurotrophic Factors. Methods in Molecular Biology (Methods and Protocols)*, Vol. **846** (Skaper S., ed), pp. 295–303. Humana Press, New York City, NY.
- Falzone T. L., Gelman D. M., Young J. I., Grandy D. K., Low M. J. and Rubinstein M. (2002) Absence of dopamine D4 receptors results in enhanced reactivity to unconditioned, but not conditioned, fear. *Eur. J. Neurosci.* **15**, 158–164.
- Falzone T. L., Stokin G. B., Lillo C., Rodrigues E. M., Westerman E. L., Williams D. S. and Goldstein L. S. B. (2009) Axonal stress kinase activation and tau misbehavior induced by kinesin-1 transport defects. *J. Neurosci.* **29**, 5758–5767.
- Falzone T. L., Gunawardena S., McCleary D., Reis G. F. and Goldstein L. S. B. (2010) Kinesin-1 transport reductions enhance human tau hyperphosphorylation, aggregation and neurodegeneration in animal models of tauopathies. *Hum. Mol. Genet.* **19**, 4399–4408.
- Gerfen C. R. and Surmeier D. J. (2011) Modulation of striatal projection systems by dopamine. *Annu. Rev. Neurosci.* **34**, 441–466.
- Gerfen C. R., Engber T. M., Mahan L. C., Sussel Z. V. I., Chase T. N., Monsma F. J. and Sibley D. R. (1990) D1R and D2R dopamine receptor-regulated gene expression of striatonigral and striatopallidal neurons. *Science* **134**, 1429–1432.
- Glater E. E., Megeath L. J., Stowers R. S. and Schwarz T. L. (2006) Axonal transport of mitochondria requires miltin to recruit kinesin heavy chain and is light chain independent. *J. Cell Biol.* **173**, 545–557.
- Kaether C., Skehel P. and Dotti C. G. (2000) Axonal membrane proteins are transported in distinct carriers: a two-color video microscopy study in cultured hippocampal neurons. *Mol. Biol. Cell* **11**, 1213–1224.
- Kamal A., Stokin G. B., Yang Z., Xia C. H. and Goldstein L. S. (2000) Axonal transport of amyloid precursor protein is mediated by direct binding to the kinesin light chain subunit of kinesin-1. *Neuron* **28**, 449–459.
- Kanai Y., Okada Y., Tanaka Y., Harada A., Terada S. and Hirokawa N. (2000) KIF5C, a novel neuronal kinesin enriched in motor neurons. *J. Neurosci.* **20**, 6374–6384.
- Kelly M. A., Rubinstein M., Phillips T. J. *et al.* (1998) Locomotor activity in D2R dopamine receptor-deficient mice is determined by

- gene dosage, genetic background, and developmental adaptations. *J. Neurosci.* **18**, 3470–3479.
- Kim K.-M., Valenzano K. J., Robinson S. R., Yao W. D., Barak L. S. and Caron M. G. (2001) Differential regulation of the dopamine D2 and D3 receptors by G protein-coupled receptor kinases and β -arrestins. *J. Biol. Chem.* **276**, 37409–37414.
- Kim-Han J. S., Antenor-Dorsey J. A. and O'Malley K. L. (2011) The parkinsonian mimetic, MPP⁺, specifically impairs mitochondrial transport in dopamine axons. *J. Neurosci.* **31**(19), 7212–7221.
- Kravitz A. V., Freeze B. S., Parker P. R. L., Kay K., Myo T., Deisseroth K. and Kreitzer A. C. (2010) Regulation of parkinsonian motor behaviors by optogenetic control of basal ganglia circuitry. *Nature* **466**, 622–626.
- Kumakura K., Nomura H., Toyoda T. *et al.* (2010) Hyperactivity in novel environment with increased dopamine and impaired novelty preference in apoptosis signal-regulating kinase 1 (ASK1)-deficient mice. *Neurosci. Res.* **66**, 313–320.
- Li Y., Roy B. D., Wang W., Zhang L., Zhang L., Sampson S. B., Yang Y. and Lin D.-T. (2012) Identification of two functionally distinct endosomal recycling pathways for dopamine D2 receptor. *J. Neurosci.* **32**, 7178–7190.
- Lipkind D., Sakov A., Kafkafi N., Elmer G. I., Benjamini Y. and Golani I. (2004) New replicable anxiety-related measures of wall vs. center behavior of mice in the open field. *J. Appl. Physiol.* (1985) **97**, 347–359.
- Lisman J. E. and Grace A. A. (2005) The hippocampal-VTA loop: controlling the entry of information into long-term memory. *Neuron* **46**, 703–713.
- Lu X., Kim-Han J. S., Harmon S., Sakiyama-Elbert S. E. and O'Malley K. L. (2014) The Parkinsonian mimetic, 6-OHDA, impairs axonal transport in dopaminergic axons. *Mol. Neurodegener.* **9**, 17.
- Luque-Rojas M. J., Galeano P., Suárez J., Araos P., Santín L. J., de Fonseca F. R. and Calvo E. B. (2012) Hyperactivity induced by the dopamine D2/D3 receptor agonist quinpirole is attenuated by inhibitors of endocannabinoid degradation in mice. *Int. J. Neuropsychopharmacol.* **16**, 661–676.
- Madisen L., Zwingman T. A., Sunkin S. M. *et al.* (2010) A robust and high-throughput Cre reporting and characterization system for the whole mouse brain. *Nat. Neurosci.* **13**, 133–140.
- Matsuda W., Furuta T., Nakamura K. C., Hioki H., Fujiyama F., Arai R. and Kaneko T. (2009) Single nigrostriatal dopaminergic neurons form widely spread and highly dense axonal arborizations in the neostriatum. *J. Neurosci.* **29**, 444–453.
- Meiser J., Weindl D. and Hiller K. (2013) Complexity of dopamine metabolism. *Cell Commun. Signal.* **11**, 34.
- Migheli R., Del G. M., Spissu Y. *et al.* (2013) LRRK2 affects vesicle trafficking, neurotransmitter extracellular level and membrane receptor localization. *PLoS ONE* **8**, e77198.
- Miki H., Setou M., Kaneshiro K. and Hirokawa N. (2001) All kinesin superfamily protein, KIF, genes in mouse and human. *Proc. Natl Acad. Sci. USA* **98**, 7004–7011.
- Mink J. W. (2003) The basal ganglia and involuntary movements. *Arch. Neurol.* **60**, 1365–1368.
- Nakajima K., Yin X., Takei Y., Seog D.-H., Homma N. and Hirokawa N. (2012) Molecular motor KIF5A is essential for GABA(A) receptor transport, and KIF5A deletion causes epilepsy. *Neuron* **76**, 945–961.
- Nakamura T., Sato A., Kitsukawa T., Momiyama T., Yamamori T. and Sasaoka T. (2014) Distinct motor impairments of dopamine D1 and D2 receptor knockout mice revealed by three types of motor behavior. *Front. Integr. Neurosci.* **8**, 56.
- Pozo Devoto V. M. and Falzone T. L. (2017) Mitochondrial dynamics in Parkinson's disease: a role for α -synuclein? *Dis. Model Mech.* **10** (9), 1075–1087.
- Pozo Devoto V. M., Dimopoulos N., Alloati M. *et al.* (2017) α Synuclein control of mitochondrial homeostasis in human-derived neurons is disrupted by mutations associated with Parkinson's disease. *Sci. Rep.* **7**, 5042.
- Rassu M., Del Giudice M. G., Sanna S. *et al.* (2017) Role of LRRK2 in the regulation of dopamine receptor trafficking. *PLoS ONE* **12**, 1–22.
- Rubinstein M., Phillips T. J., Bunzow J. R. *et al.* (1997) Mice lacking dopamine D4 receptors are supersensitive to ethanol, cocaine, and methamphetamine. *Cell* **90**, 991–1001.
- Schmidt M. R., Maritzen T., Kukhtina V., Higan V. A., Doglio L., Barak N. N., Strauss H., Oschkinat H., Dotti C. G. and Haucke V. (2009) Regulation of endosomal membrane traffic by a Gadin/AP-1/ kinesin KIF5 complex. *Proc. Natl Acad. Sci.* **106**, 15344–15349.
- Setou M., Nakagawa T., Seog D. and Hirokawa N. (2000) Kinesin superfamily motor protein KIF17 and mLin-10 in NMDA receptor-containing vesicles transport. *Science* **288**(5472), 1796–1802.
- Sharp T., Zetterström T., Ljungberg T. and Ungerstedt U. (1987) A direct comparison of amphetamine-induced behaviours and regional brain dopamine release in the rat using intracerebral dialysis. *Brain Res.* **401**, 322–330.
- Shulman J. M., De Jager P. L. and Feany M. B. (2011) Parkinson's disease: genetics and pathogenesis. *Annu. Rev. Pathol.* **6**, 193–222.
- Spillantini M. G., Schmidt M. L., Lee V. M., Trojanowski J. Q., Jakes R. and Goedert M. (1997) Alpha-synuclein in Lewy bodies. *Nature* **388**, 839–840.
- Starr B. S. and Starr M. S. (1986) Differential effects of dopamine D1R and D2R, agonists and antagonists on velocity of movement, rearing and grooming in the mouse. Implications for the roles of D1R, and D2R, receptors. *Neuropharmacology* **25**, 455–463.
- Tanaka Y., Kanai Y., Okada Y., Nonaka S., Takeda S., Harada A. and Hirokawa N. (1998) Targeted disruption of mouse conventional kinesin heavy chain, kif5B, results in abnormal perinuclear clustering of mitochondria. *Cell* **93**, 1147–1158.
- Tronche F., Kellendonk C., Kretz O., Gass P., Anlag K., Orban P. C., Bock R., Klein R. and Schütz G. (1999) Disruption of the glucocorticoid receptor gene in the nervous system results in reduced anxiety. *Nat. Genet.* **23**, 99–103.
- Twelvetrees A. E., Yuen E. Y., Arancibia-carcamo I. L. *et al.* (2011) Delivery of GABAARs to synapses is mediated by HAP1-KIF5 and disrupted by mutant huntingtin. *Neuron* **65**, 53–65.
- Usiello A., Baik J., Rougé-Pont F., Picetti R., Dierich A., LeMeur M., Piazza P. V. and Borrelli E. (2000) Distinct functions of the two isoforms of dopamine D2R receptors. *Nature* **408**, 199–203.
- Vale R. D., Reese T. S. and Sheetz M. P. (1985) Identification of a novel force-generating protein, kinesin, involved in microtubule-based motility. *Cell* **42**, 39–50.
- Volpicelli-Daley L. A. (2017) Effects of α -synuclein on axonal transport. *Neurobiol. Dis.* **105**, 321–327.
- Wang H. and Pickel V. (2002) Dopamine D2 receptors are present in prefrontal cortical afferents and their targets in patches of the rat caudate-putamen nucleus. *J. Comp. Neurol.* **442**, 392–404.
- Westlund K. N., Krakower T. J., Kwan S. W. and Abell C. W. (1993) Intracellular distribution of monoamine oxidase A in selected regions of rat and monkey brain and spinal cord. *Brain Res.* **612**, 221–230.
- Xia C. H., Roberts E. A., Her L. S., Liu X., Williams D. S., Cleveland D. W. and Goldstein L. S. B. (2003) Abnormal neurofilament transport caused by targeted disruption of neuronal kinesin heavy chain KIF5A. *J. Cell Biol.* **161**, 55–66.
- Xu M., Moratalla R., Gold L. H., Hiroi N., Koob G. F. and Graybiel A. M. (1994) Dopamine D1 receptor mutant mice are deficient in striatal expression of dynorphin and in dopamine-mediated behavioral responses. *Cell* **79**, 729–742.

Open Practices Disclosure

Manuscript Title: Neuronal KIF5b deletion induces striatum-dependent locomotor impairments and defects in membrane presentation of dopamine D2 receptors

Corresponding Author: Dr. Tomas Falzone

Articles accepted to *Journal of Neurochemistry* after 01.2018 are eligible to earn badges that recognize open scientific practices: publicly available data, material, or preregistered research plans. Please read more about the badges in our *author guidelines and Open Science Badges page*, and you can also find information on the Open Science Framework [wiki](#).

Please check this box if you are interested in participating.

To apply for one or more badges acknowledging open practices, please check the box(es) corresponding to the desired badge(s) below and provide the information requested in the relevant sections. To qualify for a badge, you must provide a URL, doi, or other permanent path for accessing the specified information in a public, open-access repository. **Qualifying public, open-access repositories are committed to preserving data, materials, and/or registered analysis plans and keeping them publicly accessible via the web in perpetuity.** Examples include the Open Science Framework ([OSF](#)) and the various Dataverse networks. Hundreds of other qualifying data/materials repositories are listed at <http://re3data.org/>. Preregistration of an analysis plan must take place via a publicly accessible registry system (e.g., [OSF](#), [ClinicalTrials.gov](#) or other trial registries in the [WHO Registry Network](#), institutional registration systems). **Personal websites and most departmental websites do not qualify as repositories.**

Authors who wish to publicly post third-party material in their data, materials, or preregistration plan must have the proper authority or permission agreement in order to do so.

There are circumstances in which it is not possible or advisable to share any or all data, materials, or a research plan publicly. For example, there are cases in which sharing participants' data could violate confidentiality. If you would like your article to include an explanation of such circumstances and/or provide links to any data or materials you have made available—even if not under conditions eligible to earn a badge—you may write an alternative note that will be published in a note in the article. Please check this box if you would like your article to include an alternative note and provide the text of the note below:

Alternative note:

Open Data Badge

1. Provide the URL, doi, or other **permanent path** for accessing the data in a **public, open-access repository**:

Confirm that there is sufficient information for an independent researcher to reproduce **all of the reported results**, including codebook if relevant.

Confirm that you have registered the uploaded files so that they are **time stamped** and cannot be age.

Open Materials Badge

1. Provide the URL, doi, or other **permanent path** for accessing the materials in a **public, open-access repository**:

Confirm that there is sufficient information for an independent researcher to reproduce **all of the reported methodology**.

Confirm that you have registered the uploaded files so that they are **time stamped** and cannot be age.

Preregistered Badge

1. Provide the URL, doi, or other **permanent path** to the registration in a **public, open-access repository***:

2. Was the analysis plan registered prior to examination of the data or observing the outcomes? If no, explain.**

No

3. Were there additional registrations for the study other than the one reported? If yes, provide links and explain.*

No


*No badge will be awarded if (1) is not provided, **or** if (3) is answered “yes” without strong justification

**If the answer to (2) is "no," the notation DE (Data Exist) will be added to the badge, indicating that registration postdates realization of the outcomes but predates analysis.

By signing below, authors affirm that the above information is accurate and complete, that any third-party material has been reproduced or otherwise made available only with the permission of the original author or copyright holder, and that publicly posted data do not contain information that would allow individuals to be identified without consent.

Date: **11, December, 2018** _____

Name: **__Tomas Falzone** _____

Signature: _____  **TOMAS FALZONE .**